Optical and ODMR Investigations of the Lowest Excited Triplet State of Dinaphtho-(2′.3′:1.2); (2″.3″:6.7)-pyrene

Chr. Bräuchle, H. Kabza, and J. Voitländer

Institute of Physical Chemistry, University of Munich, West Germany

Z. Naturforsch. **34a**, 6–12 (1979); received June 23, 1978

Dedicated to Prof. Dr. G.-M. Schwab on his 80th birthday

On the basis of the phosphorescence spectrum of dinaphtho-(2′.3′:1.2); (2″.3″:6.7)-pyrene in n-dodecane (Shpolskii matrix) at $T = 1.3$ K a site and vibrational analysis was performed. With the help of ODMR measurements the symmetries of the vibrational bands were determined. In this way for most of the normal modes an assignment of the type of vibration became feasible. Because of their different zero-field splittings (ZFS) five sites could be identified. The signs of the ZFS parameters as well as the kinetic rate constants of population and depopulation of the zero-field levels (ZFL) of T_1 were determined. Like the ZFS the kinetic rate constants too were different for each site reflecting different interaction of the molecules with the host matrix. Radiative and radiationless processes are discussed in terms of spin-orbit coupling (SOC).

1. Introduction

Aromatic hydrocarbons often serve as model systems for photophysical processes [1]. Of particular interest are the spin-forbidden transitions between the singlet system and the zero-field levels (ZFL's) of the lowest excited state T_1. The magnetic dipole-dipole-interaction of the two unpaired triplet electrons causes the splitting of the state T_1 into the three ZFL's in the absence of an external magnetic field. This zerofield-splitting (ZFS) is of the order of 0.1 cm^{-1}—0.01 cm^{-1}.

By means of the Optical Detection of Magnetic Resonance (ODMR) technique [2] the ZFS as well as the kinetics of the ZFL's can be observed quite conveniently. This method combines the high sensivity of optical detection with the good selectivity of ESR. Further it allows a relatively detailed interpretation of the phosphorescence spectra.

We intend to apply the wide scope of the ODMR technique to investigate a number of aromatic molecules containing pyrene as a common basic structure and showing different degrees of annelation. Varying numbers of benzene rings are condensed in differing positions of the pyrene skeleton [3]. In this way the influence of structure and degree of annelation on the ZFS and the dynamics of the ZFL's of T_1 shall be studied. The triplet state of a few pure aromatic molecules has been investigated by ODMR [4–6]. However, their number is small as compared to hetero- and substituted aromatic molecules [2] and the selection has not been very systematic. It seems promising therefore, to engage in such an investigation programme which — as outlined above — should yield information on the influence of structure and degree of annelation on triplet parameters by taking a series of pyrene derivatives as an example.

In this communication we shall present the first results for a typical representative of this class of molecules, the dinaphtho-(2′.3′:1.2); (2″.3″:6.7)-pyrene (DNP).

Reprint requests to Prof. Dr. J. Voitländer, Institut für Physikalische Chemie, Universität München, Sophienstraße 11, D-8000 München 2.

2. Experimental

2.1. Apparatus

The ODMR apparatus has been described before [6]. With it the phosphorescence spectrum at 1.3 K could be recorded. Weak phosphorescence and overlap of intense fluorescence necessitated the use of a light chopper in the excitation path. The chopping frequency was 800 Hz. The 313 nm Hg-line was selected for excitation. The bandwidth of the emission monochromator was adjusted to 1 cm^{-1}.

2.2. Material

The pure DNP [3] was dissolved in highly pure n-dodecane serving as a Shpolskii matrix. Concentrations were 10^{-4} mole/l or less. The samples were degassed and filled into quartz vials which were sealed off under vacuum. Luminescence spectra did not change during the course of the measurements indicating the photostability of the DNP-molecule.

3. Results

3.1. Optical Properties

Figure 1 shows the phosphorescence spectrum [7] of DNP in n-dodecane at 1.3 K. The high resolution which was not limited by the apparatus, enabled us to do an analysis of sites and vibrational bands. The vibrational analysis is shown in Table 1 while the site analysis is contained in Tables 1 and 2.

The occurrence of sites when molecules are embedded in Shpolskii matrices is a well known phenomenon [8—9]. Each of these sites possesses

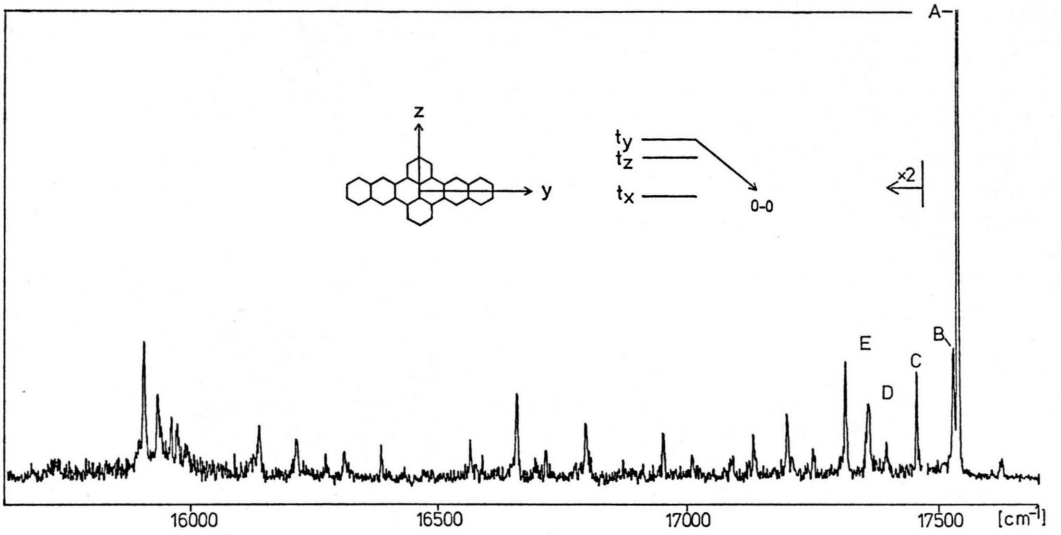

Fig. 1. Phosphorescence spectrum of dinaphtho-(2′.3′:1.2); (2″.3″:6.7)-pyrene in n-dodecane at 1.35 K.

Table 1. Analysis of the phosphorescence spectrum of dinaphtho-(2′.3′:1.2):(2″.3″:6.7)-pyrene in n-dodecane.

Int.	ν [cm^{-1}]	$\Delta\nu$ [cm^{-1}]	Possible assignment	Symmetry	k_y^r	k_z^r	k_x^r
vvs	17538		Site A, 0—0		1.00	0.06	0.02
s	17525	13	Site B, 0—0		1.00	0.08	0.04
w	17451	87	Site C, 0—0		1.00	0.11	0.05
vvw	17396	142	Site D, 0—0				
w	17358	180	Site E, 0—0		1.00	0.09	0.04
w	17313	225	$\nu_1 = 225$	a_g	1.00	0.12	0.06
vvw	17250	288	$\nu_2 = 288$				
vw	17197	341	$\nu_3 = 341$	b_{3g}	0.21	1.00	0.10
vvw	17127	411	$\nu_4 = 411$	a_g	1.00	0.21	0.09
vvw	17088	450	$2 \times \nu_1 = 450$				
vvw	17008	530	$\nu_5 = 530$				
vvw	16947	591	$\nu_6 = 591$	a_g	1.00	0.16	0.07
vw	16793	745	$\nu_7 = 745$	b_{2g}	0.34	1.00	0.08
vvw	16716	822	$\nu_8 = 822$				
w	16659	879	$\nu_9 = 879$	b_{2g}	0.36	1.00	0.10
vvw	16562	976	$\nu_{10} = 976$	b_{2g}	0.31	1.00	0.09
vvw	16383	1155	$\nu_{11} = 1155$	b_{1g}	1.00	0.60	0.19
vvw	16311	1227	$\nu_{12} = 1227$	b_{3g}	0.17	1.00	0.10
vvw	16274	1264	$\nu_2 + \nu_{10} = 1264$				
vvw	16210	1328	$2 \times \nu_1 + \nu_9 = 1329$	b_{2g}	1.00	0.42	0.09
vw	16135	1403	$\nu_{13} = 1403$, $\nu_1 + 2\nu_6 = 1407$	a_g	1.00	0.22	0.07
vvw	15992	1546	$3 \times \nu_1 + \nu_9 = 1554$				
vw	15967	1571	$\nu_{12} + \nu_3 = 1568$	a_g	1.00	0.23	0.07
vw	15957	1581	$\nu_{14} = 1581$	b_{2g}	1.00	0.40	0.08
vw	15926	1612	$\nu_{15} = 1612$	b_{3g}	0.22	1.00	0.08
w	15901	1637	$\nu_{16} = 1637$	b_{3g}	0.18	1.00	0.07

Table 2. Energies of T_1 and ZFS-parameters D and E in the different sites of dinaphtho-(2′.3′:1.2);(2″.3″:6.7)-pyrene/n-dodecane.

Site	E_{T_1} [cm^{-1}]	D [MHz] $\pm$ 1 MHz	E [MHz] $\pm$ 1 MHz
A	17538	2750.5	385.5
B	17525	2735.5	392.5
C	17451	2719	405
D	17396	2710	402
E	17358	2697	400

its own phosphorescence spectrum. The experimentally recorded spectrum then is a superposition of a corresponding number of identical phosphorescence spectra which are shifted in energy relative to each other. Since each band shows the same multiplet structure, analysis of the spectrum is simple and straightforward, even if there are many lines.

In the case of DNP in n-dodecane no multiplet structure is observed. A straightforward interpretation therefore would identify the bands marked C, D and E as vibrational bands of the main site A. This would seem even more plausible since lower lying bands might be explained as combinations of these fundamentals. Such an interpretation, however, would be wrong. ODMR measurements prove the bands B, C, D and E to be 0—0-bands of further sites.

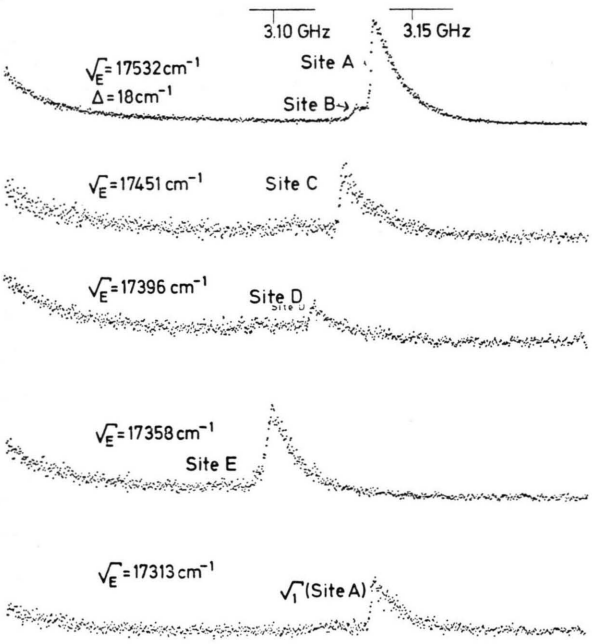

Fig. 2. ODMR transitions between the two outer sublevels t_y and t_x in the five sites and in the first vibrational band of site A (bottom).

The ZFS of T_1 and the position of the 0—0 band depend on the interaction between molecules and matrix in the various sites. Figure 2 shows the ODMR-transitions between the two outer ZFL's in the bands indicated. From the difference in resonance frequencies it follows that the bands marked B, C, D and E are the 0—0-bands of 4 sites. The first vibronic band of site A is the one at 17313 cm^{-1}.

In a case like that of DNP/n-dodecane where the 0—0-band (17538 cm^{-1}) is much more intense than all other vibronic bands, sites with less radiative intensity can only be observed in their 0—0-bands. The expected multiplet structure will not be observed because of lacking intensity and optical measurements alone may lead to an incorrect interpretation of the spectrum.

Sometimes it is possible in such a case to recognize a site through its metastability [8]. This can be observed if the relative intensities of the bands are different for fast and slow cooling of the sample. For DNP/n-dodecane, however, sites A, B, C and D proved to be thermally stable and cannot be identified as sites by varying the cooling rate.

Table 1 shows the resulting vibrational analysis of the phosphorescence spectrum of DNP. The possible assignments listed in Table 1 together with the symmetry of the vibronic bands will be discussed in Section 3.2. The symmetry of the vibronic bands can be determined from a comparison [10] of the relative radiative rate constants k_y^r, k_z^r and k_x^r and the group-theoretical analysis of the phosphorescence mechanisms. This analysis is summarized schematically in Table 4. The relative radiative rate constants were measured by means of MIDP-experiments [11] in the phosphorescence bands with sufficient intensity. 4—6 individual measurements with a high number of scans were taken in each band so the error margin does not exceed $\pm 10\%$. These accurate radiative rate constants were necessary especially for the distinction between b_{1g} and b_{2g} vibrations as will be discussed in Section 4.2.

3.2. Zero Field Splitting and Kinetic Rate Constants

Table 2 shows the ZFS of T_1 in the five sites. Until now no quantitative relationship could be

deduced between the energetic position of T_1 and its ZFS. The behaviour of the D-parameter, however, may be understood in a qualitative way. $|D|$ is a measure of the spatial separation within the molecular plane of the triplet electrons. Because of the dipolar interaction of the two electrons $|D|$ increases with decreasing average distance between them and vice versa.

From the experimental results in Table 2 it can be seen that $|D|$ increases for larger triplet energy differences $T_1 - S_0$.

It is known [12] that for aromatic hydrocarbons in n-alcanes the absorption spectra are redshifted as compared to those in the gas phase. Since solute as well as solvent are non-polar the interactions causing this spectral shift are mainly London dispersive forces.

Thus the spectral shift of $T_1 - S_0$ from site A through site E as indicated in Table 2 seems to reflect an increase in interaction strength from site A through site E. With this an energetically more favourable average separation of the two electrons seems possible as shown by the decrease of $|D|$, due to the increasing influence of the solvent on the molecule's electronic structure.

Table 3 presents the kinetic data of population and depopulation of the ZFL's of T_1. They were determined by means of MIDP-experiments at 1.3 K where SLR could be neglected. The latter was confirmed by measuring the temperature dependence of the slowest decay rate k_x. Below 1.6 K k_x remained constant within experimental error while above that temperature a slow increase could be seen. So the kinetic rate constants in Table 3 are the „true" kinetic rate constants of DNP/n-dodecane.

The notation used is as follows: k_i is the total decay rate of ZFL t_i of T_1 to the ground state S_0; K_i is the ISC rate for the population of t_i from S_1, and N_i denotes the stationary equilibrium population ratios.

The decay rate constants were determined for the sites A, B, C and E, whereas the weak intensity of site D precluded reliable measurements. For the same reason the ISC rates K_i and the relative population numbers N_i could not be determined in sites B, C, D and E (see Table 3).

4. Discussion

4.1. Signs of $|D|$ and $|E|$ and Symmetry of T_1

The axis system was chosen according to Mulliken for D_{2h} molecules as indicated in Figure 1. In this system the Hamiltonian for the ZFS can be written in the form:

$$H_{ss} = D(S_x^2 - 2/3) + E(S_y^2 - S_z^2) .$$

For aromatic molecules it is known [13—15] that the out-of-plane level t_x is the lowest in energy and therefore $D > 0$.

A Hückel calculation [16] gave $^3B_{1u}$ orbital symmetry for T_1 of DNP. From the group theoretical matrix elements listed in Table 4 then it follows that radiative intensity of the 0—0-band comes only from t_y. The MIDP experiments in the 0—0-band showed that by inducing the $|D| + |E|$ transition and so repopulating the top ZFL the highest radiative rate constant was obtained; by inducing the $|D| - |E|$ transition and so measuring the radiative rate constant of the inner ZFL a markedly lower radiative rate constant was obtained. That means that the energetic order of the two in-plane levels must be $t_y > t_z$. In the axis system chosen the signs of D and E follow from the Hamiltonian as $D > 0$ and $E < 0$.

4.2. Radiative Decay of T_1 and Vibrational Bands

If the orbital symmetry of T_1 is known the radiative decay mechanisms of the 3 ZFL's into the vibrational bands of the ground state S_0 can be determined with the help of group-theoretical analysis [15, 17]. With the four mechanisms [18]

Table 3. Kinetic rate constants for the three ZFL's of T_1 of dinaphtho-(2′.3′:1.2):(2″.3″:6.7)-pyrene/*n*-dodecane.

Site	k_y [s^{-1}]	k_z [s^{-1}]	k_x [s^{-1}]	K_y	K_z	K_x	N_y	N_z	N_x
A	1.97 ± 0.06	1.26 ± 0.15	0.158 ± 0.01	0.22	1.00	0.03	0.14	1.00	0.24
B	2.04 ± 0.08	1.41 ± 0.2	0.23 ± 0.021						
C	2.30 ± 0.09	1.67 ± 0.22	0.23 ± 0.015						
E	2.22 ± 0.12	1.53 ± 0.2	0.23 ± 0.02						

Table 4. Group theoretical matrix elements of the different SOC mechanisms for the lowest excited triplet state of a D_{2h} molecule with $^3B_{1u}$ orbital symmetry.

$^3B_{1u}(\pi\pi^*)$	$\langle T_1{}^u \vert H_{SO} \vert S_n\rangle\langle S_n \vert \hat{D} \vert S_0\rangle$ direct SOC	$\langle T_1{}^u \vert \frac{\partial H_{SO}}{\partial Q} \vert S_n\rangle\langle S_n \vert \hat{D} \vert S_0\rangle$ spin-vibronic coupling
$t_y(b_{2g})$	$^3B_{1u} \overset{SOC}{\sim\!\sim} {}^1B_{3u}(\sigma\pi^*) \overset{(x)}{\longleftrightarrow} {}^1A_g$	$^3B_{1u} \sim\!\sim b_{2g} \otimes a_g \sim\!\sim {}^1B_{3u}(\sigma\pi^*) \overset{(x)}{\longleftrightarrow} {}^1A_g$
$t_z(b_{1g})$	—	$^3B_{1u} \sim\!\sim b_{1g} \otimes b_{3g} \sim\!\sim {}^1B_{3u}(\sigma\pi^*) \overset{(x)}{\longleftrightarrow} {}^1A_g$
$t_x(b_{3g})$	three-centre contribution	$^3B_{1u} \sim\!\sim b_{3g} \otimes b_{1g} \sim\!\sim {}^1B_{3u}(\sigma\pi^*) \overset{(x)}{\longleftrightarrow} {}^1A_g$
$^3B_{1u}(\pi\pi^*)$	$\langle T_1{}^u \vert H_{S_0} \vert S_m\rangle\langle S_m \vert \frac{\partial H_e}{\partial Q} \vert S_n\rangle\langle S_n \vert \hat{D} \vert S_0\rangle$ SOC with vibr. coupling in the singlet manifold	$\langle T_1{}^u \vert \frac{\partial H_e}{\partial Q} \vert T_m{}^u\rangle\langle T_m{}^u \vert H_{S_0} \vert S_n\rangle\langle S_n \vert \hat{D} S_0\rangle$ SOC with vibr. coupling in the triplet manifold
$t_y(b_{2g})$	$^3B_{1u} \overset{SOC}{\sim\!\sim} {}^1B_{3u}(\sigma\pi^*)$ { $\overset{vibr.}{\sim\!\sim}_{b_{2g}} {}^1B_{1u}(\pi\pi^*) \overset{(z)}{\longleftrightarrow} {}^1A_g$; $\overset{}{\sim\!\sim}_{b_{1g}} {}^1B_{2u}(\pi\pi^*) \overset{(y)}{\longleftrightarrow} {}^1A_g$; $\overset{}{\sim\!\sim}_{a_g} {}^1B_{3u}(\sigma\pi^*) \overset{(x)}{\longleftrightarrow} {}^1A_g$ }	$^3B_{1u}$ { $\overset{vibr.}{\sim\!\sim}_{b_{2g}} {}^3B_{3u}(\sigma\pi^*) \overset{SOC}{\sim\!\sim} {}^1B_{1u}(\pi\pi^*) \overset{(z)}{\longleftrightarrow} {}^1A_g$; $\overset{}{\sim\!\sim}_{b_{1g}} {}^3A_u(\sigma\pi^*) \sim\!\sim {}^1B_{2u}(\pi\pi^*) \overset{(y)}{\longleftrightarrow} {}^1A_g$; $\overset{}{\sim\!\sim}_{a_g} {}^3B_{1u}(\pi\pi^*) \sim\!\sim {}^1B_{3u}(\sigma\pi^*) \overset{(x)}{\longleftrightarrow} {}^1A_g$ }
$t_z(b_{1g})$	$^3B_{1u} \overset{SOC}{\sim\!\sim} {}^1A_u(\sigma\pi^*)$ { $\overset{vibr.}{\sim\!\sim}_{b_{1g}} {}^1B_{1u}(\pi\pi^*) \overset{(z)}{\longleftrightarrow} {}^1A_g$; $\overset{}{\sim\!\sim}_{b_{2g}} {}^1B_{2u}(\pi\pi^*) \overset{(y)}{\longleftrightarrow} {}^1A_g$; $\overset{}{\sim\!\sim}_{b_{3g}} {}^1B_{3u}(\sigma\pi^*) \overset{(x)}{\longleftrightarrow} {}^1A_g$ }	$^3B_{1u}$ { $\overset{vibr.}{\sim\!\sim}_{b_{1g}} {}^3A_u(\sigma\pi^*) \overset{SOC}{\sim\!\sim} {}^1B_{1u}(\pi\pi^*) \overset{(z)}{\longleftrightarrow} {}^1A_g$; $\overset{}{\sim\!\sim}_{b_{2g}} {}^3B_{3u}(\sigma\pi^*) \sim\!\sim {}^1B_{2u}(\pi\pi^*) \overset{(y)}{\longleftrightarrow} {}^1A_g$; $\overset{}{\sim\!\sim}_{b_{3g}} {}^3B_{2u}(\pi\pi^*) \sim\!\sim {}^1B_{3u}(\sigma\pi^*) \overset{(x)}{\longleftrightarrow} {}^1A_g$ }
$t_x(b_{3g})$	three-centre contribution	$^3B_{1u} \overset{vibr.}{\sim\!\sim}_{b_{1g}} {}^3A_u(\sigma\pi^*) \overset{SOC}{\sim\!\sim} {}^1B_{3u}(\sigma\pi^*) \overset{(x)}{\longleftrightarrow} {}^1A_g$

(1) direct spin-orbit coupling (SOC), SOC with vibronic coupling in the (2) singlet and (3) triplet manifold and (4) spin-vibronic coupling the decay scheme as pictured in Table 4 is obtained for a $^3B_{1u}$ state of the D_{2h} point group. In this decay scheme only those SOC mechanisms have been taken into account which connect $\pi\pi^*$ states with $\pi\sigma^*$ or $\sigma\pi^*$ states and in this way lead to important one-centre integrals ($\pi\sigma^*$ and $\sigma\pi^*$ states both will be denoted as $\sigma\pi^*$ in the following). So the only vibrational bands to be observed in the phosphorescence spectrum aside from the 0—0-band must have the symmetry a_g, b_{1g}, b_{2g} or b_{3g}. By comparison of the radiative intensities according to Table 4 with those obtained experimentally the symmetries and radiative mechanisms of the vibrational bands can be determined.

However, the distinction between the two out-of-plane vibrations b_{1g} and b_{2g} proves to be rather difficult considering the radiative rate constants alone. b_{1g} and b_{2g} both obtain their radiative intensity mainly from t_y and t_z. On the other hand b_{1g} vibrational bands should be the only ones to get intensity from t_x too. This is due to spin-vibronic coupling of t_x with a $^1B_{3u}(\sigma\pi^*)$ state through a b_{1g} vibration and SOC with vibronic (b_{1g}) coupling in the triplet manifold

$$\{{}^3B_{1u} \overset{vibr}{\sim\!\sim} {}^3A_u(\sigma\pi^*) \overset{SOC}{\sim\!\sim} {}^1B_{3u}(\sigma\pi^*)\},$$

both mechanisms leading to one-centre integrals of the SOC. According to Albrecht [18], however, spin-vibronic coupling is smaller than the mechanisms (1)—(3) and the magnitude of SOC matrix elements between two $\sigma\pi^*$ states as compared to those between $\pi\pi^*$ and $\sigma\pi^*$ states [19] is unknown. Still, because of their one-centre contributions the SOC matrix elements between two $\sigma\pi^*$ states should be greater than those between two $\pi\pi^*$ states. Consequently one should be able to identify b_{1g} vibrational bands as the only ones that get little but detectable intensity from t_x.

To date this possibility to distinguish between the b_{1g} and b_{2g} vibrations has not been utilized [10, 15, 17]. In the case of DNP reported here it is of considerable importance. Due to extremely weak phosphorescence intensity in the single vibrational bands and depolarization effects in our optical system photoselection experiments failed. Such experiments could have helped in the distinction of the two vibrational symmetries through the

different polarizations of radiation from t_y and t_z in b_{1g} and b_{2g} vibrational bands. Without the photoselection technique applicable there remains only the k_x^r-rate to distinguish between the b_{1g} and b_{2g} symmetries.

Table 1 summarizes the experimentally determined relative radiative rate constants k_y^r, k_z^r and k_x^r. From the experimental data it follows that the vibrational band at 16383 cm^{-1} is the only one with a pronounced k_x^r-rate obtaining additional intensity from t_y and t_z. So according to the foregoing discussion this band is of b_{1g} symmetry and the qualitative theoretical considerations seem to be confirmed rather well.

The symmetries of the other vibrational bands follow from Table 4 and the values of k_y^r, k_z^r and k_x^r.

It is well known [20—24] that independent of their degree of annelation for pure aromatic hydrocarbons there exist quite pronounced frequency regions for various types of vibrations. If this information is combined with the results of the symmetry analysis based on the ODMR measurements it is possible to arrive at some conclusions concerning the type of vibration giving rise to each single phosphorescence band.

The normal modes v_1—v_6 which are of a_1 or b_{3g} symmetry and accordingly correspond to vibrations within the molecular plane, all belong to the region of C—C bending (parallel: ||) vibrations [20] and lead to skeletal distortions.

The normal modes v_7—v_9 can be attributed to C—H-wagging vibrations. This follows from their b_{2g} symmetry corresponding to out-of-plane vibrations and their frequency. Extensive investigations [23—27] have shown that C—H-wagging vibrations in which adjacent H-atoms oscillate in phase occur independent of the degree of annelation between 700 cm^{-1} and 900 cm^{-1}.

The normal mode $v_7 = 745$ cm^{-1} can be explained as a so called „quartet"-band [23] which has four H-atoms oscillating in phase and which can be found in the region 735 cm^{-1} — 770 cm^{-1} in IR-spectra. In the case of DNP v_7 corresponds to an in-phase oscillation of the 4 adjacent H-atoms at the outer benzene rings of the two annelated naphthalene skeletons.

The normal mode $v_8 = 822$ cm^{-1} then might correspond to a so called „trio"-CH-wagging vibration [23]. This type of vibration is observed between 750 cm^{-1} and 810 cm^{-1} in the IR-spectra.

The „solo"-CH-wagging vibrations [23] occurring between 860 cm^{-1}—900 cm^{-1} could explain the normal mode $v_9 = 879$ cm^{-1} in the DNP-molecule. This band is relatively intense corresponding to the four independent „solo"-oscillators in DNP.

The vibrations $v_{10} = 976$ cm^{-1}, $v_{11} = 1155$ cm^{-1} and $v_{12} = 1227$ cm^{-1} have been attributed to normal modes although they could be explained as combinations. This has not been done since these combinations do not seem to be realistic because of symmetry and intensity reasons. According to their symmetry the normal modes v_{10} and v_{11} probably are C—H-bending (perpendicular: $\perp$) vibrations whereas v_{12} is a C—H-bending(||) vibration typical of this frequency region [20].

Another typical vibration in aromatic molecules is the so called gamma-C—C stretching vibration [6, 7, 22] which has a_1-symmetry and is located between 1350 cm^{-1} and 1400 cm^{-1}. The vibration $v_{13} = 1403$ cm^{-1} in DNP might be attributed to such a gamma vibration. However, a combination is also possible. A clear distinction is not feasible on the basis of the presently available experimental data.

The normal modes v_{15} and v_{16} unambiguously can be identified as C—C stretching vibrations [20] whereas the frequency of v_{14} seems too high for a b_{2g}-vibration and no particular type of vibration is ascribed to this band.

4.3. Radiationless Processes

It has been maintained in numerous communications [5, 6] that in the case of molecules showing very weak phosphorescence intensity the total decay rates k_i in good approximation can be taken as the nonradiative decay rates k_i^n. The same arguments also apply in the case of DNP.

So the radiationless decay and the population of the three ZFL's can be described by means of the total decay rates k_i and the ISC-rates K_i, and a behaviour typical of aromatic molecules becomes apparent [5, 6, 19, 25]: The two in-plane ZFL's are characterized by distinctly faster radiationless processes than the out-of-plane level. For the sites A, B, C and E a ratio of $15 \leqq (k_y + k_z)/k_x \leqq 20$ is obtained in good agreement with theoretical calculations [19] which give values of 10—30 for pure aromatic hydrocarbons. The differences in radiationless decay rates between in-plane and out-of-plane ZFL's are explained by the fact that for the in-plane levels one-centre integrals are

obtained already in first order of SOC whereas only in second order for the out-of-plane level.

In an earlier study on coronene derivatives [6] we found that the ratio of the decay rates of in-plane and out-of-plane levels varied for the different sites and we were able to find a correlation with the molecule's planarity in the different sites.

A similar behaviour is observed here for DNP where the $(k_y + k_z)/k_x$ ratio is greatest for site A, and all other sites clearly show lower values. However, for sites B, C and E the k_z-decay rates cannot be determined with great precision because these sites are only observed in their 0—0-band where radiative intensity originates almost exclusively in t_y. Therefore an MIDP-signal of the $t_x - t_z$-transition is hard to detect. The decay of such a signal would give a much more precise value for k_z than the MIDP-analysis of $t_y - t_z$ transition signals since the decay rates of t_z and t_y are almost equal. So because of the relatively large error in the measurement of k_z conclusions following from the value of $(k_y + k_z)/k_x$ with respect to planarity of the molecules in the different sites have to be taken with some caution. Still it seems rather obvious that the difference between in-plane and out-of-plane decay rates (the difference being due to the molecular plane as a symmetry element) is clearly more pronounced in site A than in site B, C and D. Therefore planarity of the molecule seems to be better conserved in site A than in sites B, C and D.

Acknowledgement

The authors would like to thank Dr. W. Schmidt of the Institute of Organic Chemistry, University of Munich, for helpful discussions and the preparation of the matrix solutions. Support of this work as well as a grant to one of us (H.K.) from the Deutsche Forschungsgemeinschaft are gratefully acknowledged.

[1] a) J. B. Birks, Photophysics of Aromatic Molecules, Wiley-Intersci., London 1970. — b) J. B. Birks, Organic Molecular Photophysics, Vol. I and II, John Wiley, London 1973 and 1975. — c) S. P. McGlynn, T. Azumi, and M. Kinoshita, Molecular Spectroscopy of the Triplet State, Prentice Hall, Englewood Cliffs, New Jersey 1969.

[2] M. A. El-Sayed, Ann. Rev. Phys. Chem. **26**, 235 (1975).

[3] E. Clar, Polycyclic Hydrocarbons, Academic Press, London 1964, Vol. I and II.

[4] a) H. Sixl and M. Schwoerer, Z. Naturforsch. Teil A **25**, 1383 (1970). — b) M. A. El Sayed, W. R. Moomaw, and J. B. Chodak, Chem. Phys. Letters **20**, 11 (1973). — c) K. Ohno, N. Nishi, M. Kinoshita, and H. Inokuchi, Chem. Phys. Letters **33**, 293 (1975). — d) R. H. Clarke and J. M. Hayes, Chem. Phys. Letters **27**, 556 (1974). — e) R. H. Clarke, J. M. Hayes, and R. H. Hofeldt, J. Magn. Reson. **13**, 68 (1974). — f) M. Schwoerer and H. Sixl, Chem. Phys. Letters **2**, 14 (1968). — g) M. Schwoerer and H. Sixl, Z. Naturforsch. **24a**, 952 (1969). — h) D. A. Antheunis, J. Schmidt, and J. H. van der Waals, Mol. Phys. **27**, 1521 (1974).

[5] R. H. Clarke and H. A. Frank, J. Chem. Phys. **65**, 39 (1976).

[6] Chr. Bräuchle, H. Kabza, and J. Voitländer, Chem. Phys., **32**, 63 (1978).

[7] W. Schmidt and E. Clar, Tetrahedron Lett., to be published.

[8] a) C. Pfister, Chem. Phys. **2**, 171, 181 (1973). — b) M. Lamotte, A. M. Merle, J. Joussot-Dubien, and F. Dupuy, Chem. Phys. Letters **35**, 410 (1975). — c) A. M. Merle, M. Lamotte, S. Risemberg, C. Hauw, J. Gaultier, and J. Ph. Grivet, Chem. Phys. **22**, 207 (1977) and references in a), b), and c).

[9] A. M. Merle, W. M. Pitts, and M. A. El-Sayed, Chem. Phys. Lett. **54**, 211 (1978).

[10] a) M. A. El-Sayed, D. V. Owens, and D. S. Tinti, Chem. Phys. Letters **6**, 395 (1970). — b) A. H. Francis and C. B. Harris, J. Chem. Phys. **57**, 1050 (1972).

[11] J. Schmidt, D. A. Antheunis, and J. H. van der Waals, Mol. Phys. **22**, 1 (1971).

[12] M. Lamotte, R. Lesclaux, A. M. Merle, and J. Joussot-Dubien, Faraday Disc. Chem. Soc. **58**, 253 (1975).

[13] J. S. Brinen and M. K. Orloff, J. Chem. Phys. **45**, 4747 (1966).

[14] M. J. Buckley, C. B. Harris, and R. M. Panos, J. Amer. Chem. Soc. **94**, 3692 (1972).

[15] C. R. Chen and M. A. El-Sayed, Chem. Phys. Letters **10**, 307 (1971).

[16] W. Schmidt, private communications, Institute of Organic Chemistry, University of Munich.

[17] M. A. El-Sayed, in Excited States, Vol. I, ed. E. C. Lim, Academic Press, New York 1974, p. 35.

[18] A. C. Albrecht, J. Chem. Phys. **38**, 354 (1963).

[19] a) F. Metz, S. Friedrich, and G. Hohlneicher, Chem. Phys. Letters **16**, 353 (1972). — b) F. Metz, Chem. Phys. Letters **22**, 186 (1973).

[20] a) E. R. Lippincot and E. J. O'Reilly jr., J. Chem. Phys. **23**, 238 (1955). — b) The Aldrich Library of Infrared Spectra, Vol. Aromatic Hydrocarbons (Aldrich Chemical Company 1970).

[21] H. Luther and H.-J. Drewitz, Z. Elektrochem. **66**, 546 (1962).

[22] J. W. Sidman, J. Chem. Phys. **25**, 122 (1956).

[23] M. P. Groenewege, Colloquium Spectroscopicum Internationale VI, Amsterdam 1956, Pergamon Press London, p. 579.

[24] C. G. Cannon and G. B. B. M. Sutherland, Spectrochim. Acta **4**, 373 (1951).

[25] a) B. R. Henry and W. Siebrand, J. Chem. Phys. **54**, 1072 (1971). — b) V. Lawetz, G. Orlandi, and W. Siebrand, J. Chem. Phys. **56**, 4058 (1972).